Monolithic InAs QDs based Active-Passive Integration for Photonic Integrated Circuits

A. Enderson [1,*], P. Mishra [1,*], Z. Cao[1], F. T. Albeladi [1, 2], S. Gillgrass [1], B-P. Ratiu[1], N. Peng[3], M. Tang [4], H-Y. Liu [4], S. Shutts [1], and P. M. Smowton [1]

1. School of Physics and Astronomy, Cardiff University, The Parade, Cardiff. CF24 3AA. UK.
2. Physics Department, Faculty of Science, University of Jeddah, Jeddah 21589, Saudi Arabia.
3. Surrey Ion Beam Centre, University of Surrey, Guildford, Surrey, UK.
4. Department of Electrical Engineering, University College London, London, UK.
*Authors contributed equally
EndersonA@Cardiff.ac.uk; mishrap3@Cardiff.ac.uk

2023 IEEE Photonics Conference (IPC) | 979-8-3503-4722-7/23/$31.00 ©2023 IEEE | DOI: 10.1109/IPC57732.2023.10360634

***Abstract*— We demonstrated 20 nm relative blue shifted III-V passive waveguides monolithically integrated with InAs QDs active laser diode emitting at 1290 nm through selective area proton implantation and post-annealing method. This work is promising for low-loss monolithic Photonic Integrated Circuits.**

Keywords—lasers, quantum dots, photonic integration

I. Introduction

Photonic Integrated Circuits (PICs) are garnering significant attention from the research community due to their wide-ranging applications across various sectors, including telecommunications, data communications, healthcare, and artificial intelligence. Further developments of PICs rely on the efficient integration of active optical components with other passive components. Recently, microtransfer printing of III-V to achieve integration with amorphous Si/Si_3N_4 waveguide [1]; adhesive bonding of III-V onto patterned SOI [2]; selective regrowth using MOCVD have been proposed to integrate active devices with passive Si_3N_4 waveguides [3]. However, these heterogeneous integration or regrowth methods are complicated and large refractive index difference between SiN waveguides and electrically pumped III-V laser diodes pose challenges of efficient integration. Alternatively, postgrowth selective area intermixing offers the advantage of seamless integration and is a low loss coupling route for PICs without resorting to regrowth or heterogeneous integration methods. Recent work on the InAs quantum dots (QDs) laser establishes the viability and promises its use as a gain material for the implementation of PICs [4]. However, investigation on the selective area intermixing on InAs QDs based gain material for implementing PICs needs attention.

Thus, in this work, we present a selective area ion implantation approach for realizing on-chip III-V based passive waveguides integrated with an active InAs QDs based laser section with the emission wavelengths in the O-band. Specifically, proton bombarded with the optimized energy 300 KeV and dose of 5×10^{12} cm^{-2} in selective areas on the chip by using a standard photolithography-based photoresist mask. Such a proton implantation process causes crystal defects in the InAs QDs based gain material thus causing complete quenching of optical emission. However, such crystal defects act as the onset of the enhanced intermixing as compared to the unimplanted region of the chip during crystal repair process. We successfully recovered the optical quality of the gain material through optimized rapid thermal annealing (RTA) at 635 ^{O}C and achieved enhanced intermixing in the implanted region of InAs QDs based gain material thus causing a relative blueshift of 20 nm measured using electrical injection.

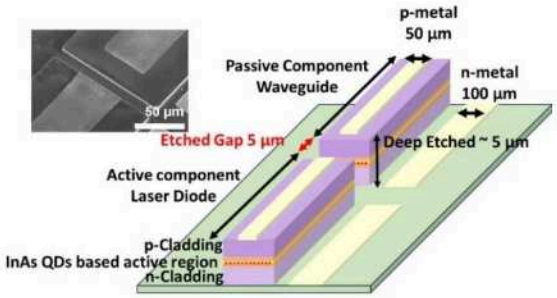

Figure 1: Schematics of monolithically integrated InAs QDs based laser and InAs QDs based passive waveguide (Inset figure shows scanning electron microscopic image of InAs QDs based active-passive integrated device).

II. Results and Discussion

Figure 1 shows the schematic of an active device with a cavity length 2 mm, coupled to a waveguide also with length 2 mm separated by an etched gap of 5 µm width; the inset figure shows a scanning electron microscopic image of the implemented device. The fabricated devices were characterised at 300 K under pulsed conditions, with a pulse width of 1000 ns and repetition rate of 5 kHz. Figure 2 shows the current-voltage (I-V) curve comparing the performance of coupled laser-waveguides with unimplanted and implanted active sections. The power output is measured as light escapes from the etched facet of the waveguide. The figure 2 inset shows the I-V and power-current density curves for an as-grown reference laser with two cleaved facets and a 2 mm cavity length. Active-passive integrated devices used in this study have two cleaved facets (at either end of the integrated device) and two etched facets (at the junction of active and passive). When compared to the as-grown laser I-V curve the voltage has increased significantly for integrated devices. The active (implanted)-passive (implanted) also has relatively higher turn on voltage, mainly attributed to the implantation process.

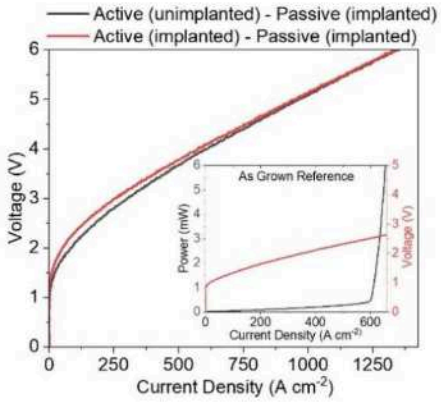

Figure 2: I-V curve comparing integrated laser-waveguides with unimplanted and implanted active regions. The insert figure shows the P-I and I-V curves for an as-grown reference laser.

The implanted device has a noticeably increased threshold current density in comparison with the unimplanted as shown in Figure 3, which compliments the I-V results. This is to be expected due to the defects caused by ion implantation and would not impact performance in applications where implanted sections would not be used as active components. In comparison with the data for the as-grown laser shown in the inset figure 2, the threshold current density for the unimplanted is also increased.

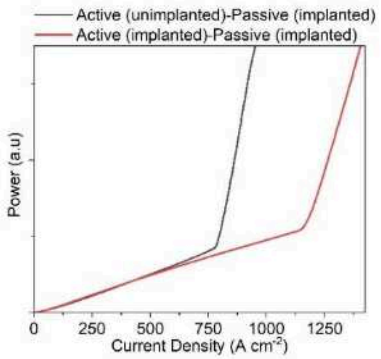

Figure 3: Power-current density curve comparing coupled laser-waveguides with unimplanted and implanted active regions.

Increase in the threshold current density and resistance in the active-passive devices as compared to that of reference device are mainly attributed to the high temperature 635 ^{O}C annealing step used, increased from a 380 ^{O}C maximum contact annealing temperature used for the reference device. In addition, difference in the facet schemes i.e., combination of cleaved-etched facets in the active-passive integrated devices are also responsible for relative increase of threshold current density and reduction in the optical power as compared to that of the as grown reference laser device with two cleaved facets.

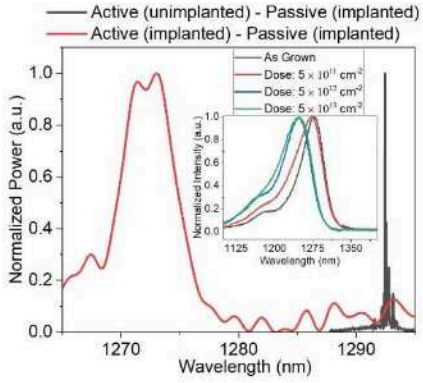

Figure 4: Wavelength measurements for integrated laser-waveguides with unimplanted and implanted active regions.

Figure 4 displays wavelength measurements taken when electrically injected above the corresponding threshold current for both the implanted and unimplanted active devices. A 20 nm relative blue shift in the wavelengths is observed between unimplanted and implanted active devices, however a band filling effect may also contribute to such blueshift as threshold current is increased. This is, however over two times the blueshift observed upon increased current density in the as grown device, with an increase from 522 (A cm^{-2}) to 3422 (A cm^{-2}) resulting in only a 9.6 nm blueshift. Additionally, we achieved a 32 nm relative blueshift (as shown in Figure 4 inset) measured using Photoluminescence (PL) during optimization of the range of proton doses (5×10^{11} cm^{-2} to 5×10^{13} cm^{-2}). Hence, obtaining a 20 nm blueshift with electrical injection in the implanted sample with respect to that of unimplanted is attributed to implantation process and RTA. Anomalous broadening with 5 nm FWHM in the spectra of the implanted device is observed and is attributed to the severe crystal defects during proton bombardments. However, achieving improved crystal recovery post proton bombardment for efficient passive components through further optimized RTA remains desirable.

In summary, we demonstrated InAs QDs based monolithic active-passive integration with a relative blueshift of 20 nm by using proton implantation and RTA operating in the O-band. This work paves the way for low-loss InAs QDs based monolithically integrated PICs.

References

[1] Beeck C. O. d., Haq B., Elsinger L., Gocalinska A., Pelucchi E., Corbett B., Roelkens G., and Kuyken B., "Heterogeneous III-V on silicon nitride amplifiers and lasers via microtransfer printing," Optica 7, 386-393 (2020)

[2] Keyvaninia, S., Muneeb, M., Stanković, S., Van Veldhoven, P. J., Van Thourhout, D., & Roelkens, G. (2013). Ultra-thin DVS-BCB adhesive bonding of III-V wafers, dies and multiple dies to a patterned silicon-on-insulator substrate. Optical Materials Express, 3(1), 35-46, 2013.

[3] Li, J., Xue, Y., Yan, Z., Han, Y., & Lau, K. M., III–V selective regrowth on SOI for telecom lasers in silicon photonics. Journal of Applied Physics, 133(13), 2023.

[4] Albeladi, F., Gillgrass, S.J., Nabialek, J., Mishra, P., Forrest, R., Albiladi, T., Allford, C.P., Deng, H., Tang, M., Liu, H. Shutts, S., and Smowton, P.M., Design and Characterisation of Multi-Mode Interference Reflector Lasers for Integrated Photonics. Journal of Physics D: Applied Physic, 2023.

Device fabrication was carried out in the cleanroom of the European Regional Development Fund (ERDF)-funded Institute for Compound Semiconductors (ICS) at Cardiff University. EPSRC funded Future Compound Semiconductor Manufacturing Hub: reference EP/P006973/1 and EPSRC funded QUDOS Programme Grant EP/T028475/1 provided essential resources for this study.